



Deposited via The University of Leeds.

White Rose Research Online URL for this paper:

<https://eprints.whiterose.ac.uk/id/eprint/223312/>

Version: Published Version

Article:

Ncube, T.R.L., Lovett, J.C., de Klerk, H.M. et al. (2025) On the Fractal Dimension of Ecotones Among African Vascular Plants. *Annals of the Missouri Botanical Garden*, 110. pp. 138-150. ISSN: 0026-6493

<https://doi.org/10.3417/2025866>

This item is protected by copyright. Reproduced with permission from the publisher.

Reuse

Items deposited in White Rose Research Online are protected by copyright, with all rights reserved unless indicated otherwise. They may be downloaded and/or printed for private study, or other acts as permitted by national copyright laws. The publisher or other rights holders may allow further reproduction and re-use of the full text version. This is indicated by the licence information on the White Rose Research Online record for the item.

Takedown

If you consider content in White Rose Research Online to be in breach of UK law, please notify us by emailing eprints@whiterose.ac.uk including the URL of the record and the reason for the withdrawal request.

ON THE FRACTAL DIMENSION OF ECOTONES AMONG AFRICAN VASCULAR PLANTS¹

Thinabakho R. L. Ncube,² Jon C. Lovett,^{3}
Helen M. de Klerk,⁴ and Cang Hui^{2,5,6}*

ABSTRACT

Ecotones are transition zones of plant species compositional turnover, with inherent fractal characteristics corresponding to the shape of boundaries between adjacent bioregions. We characterize present-day ecotones of vascular plants across mainland sub-Saharan Africa and investigate environmental factors associated with their shapes. Specifically, we explore, (1) whether a fractal dimension is appropriate for characterizing the spatial patterns of ecotones, and (2) how the fractal dimensions of present-day ecotones may vary along latitudes and reflect other environmental contrasts between adjacent bioregions. Distributions of 23,189 vascular plant species were partitioned into bioregions across mainland sub-Saharan Africa according to the nonmetric multidimensional scaling (MDS) of Jaccard dissimilarity at 20 km resolution. The optimal number of clusters was determined using K-medoids and Clustering Large Applications (CLARA) algorithms, with the clustering validity evaluated using the silhouette coefficient. The present-day ecotones were then extracted as boundaries between adjacent bioregions, and their spatial patterns measured by the box-counting fractal dimension. Using generalized additive models (GAMs), we explained the variation of the fractal dimensions of present-day ecotones by the absolute differences in mean annual precipitation, mean annual temperature, bulk density, soil clay content, soil sand content, soil organic carbon, soil pH, topographic roughness, fire frequency, human footprint, geographic extent, and latitude, separately, between two adjacent bioregions. The MDS performed reasonably well (stress = 0.057), while CLARA succeeded in partitioning seven geographically distinct clusters (0.49 silhouette

¹T. R. L. N. is grateful to the National Research Foundation of South Africa (NRF) for the Ph.D. scholarship; C. H. is supported by the NRF (grant 89967) and the Horizon Europe (101059592). We are also grateful to the Global Environment Facility SPARC project grant GEF-5810 for compiling the plant distribution dataset used in this analysis, and to the herbaria that contributed plant distribution data to the SPARC project. Without the invaluable long-term and painstaking work of herbaria carefully curating and identifying collections, this type of analysis would not be possible: A, AAH, AAS, AAU, ABH, ACOR, AD, AFS, AJOU, AK, AKPM, ALCB, ALU, AMES, AMNH, AMO, ANA, ANSM, AQP, ARAN, ARM, AS, ASDM, ASU, AUT, AV, AWH, B, BA, BAA, BAB, BABY, BACP, BAF, BAFC, BAI, BAL, BARC, BBB, BBS, BC, BCMEX, BCN, BCRU, BEREA, BESA, BG, BH, BHCB, BIO, BISH, BKF, BLA, BM, BO, BOL, BOLV, BONN, BOON, BOTU, BOUM, BPI, BR, BREM, BRI, BRIT, BRLU, BSB, BUT, C, CAMU, CAN, CANB, CANU, CAS, CATA, CATIE, CAY, CBG, CBM, CDA, CDBI, CEN, CEPEC, CESJ, CGE, CGMS, CHAM, CHAS, CHR, CHRB, CHSC, CIB, CICY, CIIDIR, CIMI, CLEMS, CLF, CMM, CNH, CNS, COA, COAH, COCA, COFC, COL, COL, COLO, CONC, CORD, CP, CPAP, CPUN, CR, CRAI, CRP, CS, CSU, CSUSB, CTES, CTESN, CU, CUVG, CUZ, CVRD, DAO, DAV, DBG, DLF, DNA, DS, DUKE, MAE, DUSS, E, EA, EAC, EAN, ECON, ECU, EIF, EIU, EKY, EMMA, ENCB, ER, ERA, ESA, ETH, F, FAA, FAU, FAUC, FCO, FCQ, FEN, FHO, FI, FLAS, FLOR, FM, FR, FSU, FTC, FUEL, FULD, FURB, G, GAT, GB, GDA, GENT, GEO, GH, GI, GLM, GMDRC, GMNHJ, GOET, GRA, GUA, GZU, H, HA, HAL, HAM, HAMAB, HAS, HAST, HASU, HB, HBC, HBR, HCIB, HGI, HGM, HIB, HIP, HO, HPL, HRCB, HRP, HSC, HSS, HU, HUA, HUA, HUAL, HUAZ, HUCP, HUEFS, HUEM, HUJ, HUSA, HUT, HYO, IAA, IAC, IAN, IB, IBGE, IBK, IBSC, IBUG, ICEL, ICESI, ICN, IEA, IEB, ILL, ILLS, INB, INEGI, INM, INPA, IPA, IPRN, IRVC, ISC, ISKW, ISU, IZAC, IZTA, JBAG, JBG, JCT, JE, JEPS, JOTR, JROH, JUA, JYV, K, KIEL, KMN, KMNH, KOR, KPM, KSTC, KTU, KU, KUN, KYO, L, LA, LAE, LAF, LAGU, LBG, LCR, LD, LE, LEB, LI, LIL, LINC, LINN, LISC, LISI, LISU, LL, LMS, LOJA, LOMA, LP, LPAG, LPB, LPD, LPS, LSU, LSM, LTB, LTR, LYJB, M, MA, MACF, MAK, MARS, MARY, MASS, MB, MBK, MBM, MBML, MCNS, MEL, MELU, MEN, MERL, MEXU, MFU, MG, MGC, MHA, MICH, MIN, MISS, MJG, MNHM, MNHN, MO, MOL, MPN, MPU, MSB, MSC, MSUN, MU, MUB, MVFA, MVFQ, MVJB, MVM, MW, MY, N, NA, NAC, NAS, NCSC, NCU, ND, NE, NH, NHM, NHMC, NHT, NLH, NMNL, NMR, NMSU, NSW, NU, NUM, NWOSU, NY, NZFRJ, O, OBI, OCLA, ODU, OKL, OKLA, OS, OSA, OSC, OSH, OULU, OXF, P, PACA, PAMP, PAR, PASA, PDD, PE, PEL, PERTH, PEUFR, PGM, PH, PKDC, PMA, POM, PORT, PR, PRC, PRE, PSU, PY, QCA, QCNE, QMEX, QRS, R, RB, REG, RELC, RFA, RIOG, RM, RNG, RSA, RYU, S, SACT, SALA, SAN, SANT, SAPS, SASK, SAV, SBBG, SBT, SCFS, SD, SDSU, SEL, SEV, SF, SFV, SGO, SI, SING, SIU, SJRP, SJSU, SLPM, SMDB, SNM, SOM, SP, SPF, SRFA, STL, STU, SUU, SUVA, SVG, SZU, TAES, TAI, TAIF, TALL, TAM, TAMU, TAN, TEF, TENN, TEPB, TEX, TI, TKPM, TNS, TO, TOYA, TRA, TRH, TROM, TRT, TU, TUB, TULS, U, UADY, UAM, UAS, UB, UBT, UC, UCR, UCS, UCSB, UCSC, UEC, UESC, UFG, UFMA, UFMT, UFP, UFRJ, UFRN, UFS, UGDA, UH, UI, UJAT, ULM, ULS, UME, UMO, UNA, UNCC, UNEX, UNITEC, UNL, UNM, UNR, UNSL, UPGB, UPNA, UPS, US, USAS, USE, USJ, USM, USNC, USP, USZ, UT, UTC, UTEP, UU, UV, UVIC, VAL, VDB, VEN, VIT, VMSL, VT, W, WAG, WELT, WH, WIS, WMNH, WOLL, WS, WTU, WU, XAL, YAMA, Z, ZMT, ZSS, and ZT.

²Centre for Invasion Biology, Department of Mathematical Sciences, Stellenbosch University, Stellenbosch 7602, South Africa.

³School of Geography, University of Leeds, Leeds LS2 9JT, United Kingdom.

⁴School of Landscape Architecture, Lincoln University, Lincoln 7647, Christchurch, New Zealand.

⁵Biodiversity Informatics Unit, African Institute for Mathematical Sciences, Cape Town 7945, South Africa.

⁶National Institute for Theoretical and Computational Sciences, Stellenbosch University, Stellenbosch 7602, South Africa.

* Author for correspondence: j.lovett@leeds.ac.uk

coefficient), from which 11 ecotones were identified, with eight characterized as true fractals but having low fractal dimensions (range: from 1.018 to 1.154). The GAM identified the difference in mean annual precipitation as significant ($P = 0.02$) for explaining the variation of the fractal dimensions of present-day ecotones with the difference in soil organic carbon near-significant ($P = 0.07$). The fractal dimensions also showed a moderate correlation with the difference in human footprint between adjacent bioregions (Spearman's $\rho = 0.619$), albeit not significant ($P = 0.11$). Overall, by spatially characterizing the present-day ecotones between different bioregions, we showed that the fractal dimension is an appropriate method for shape quantification and characterization of ecotones. We further highlighted key environmental factors that could explain the formation of present-day ecotones and thus the compositional turnover of vascular plant species across sub-Saharan Africa.

Key words: Bioregionalization, boundary detection, compositional turnover, ecotone, fractal dimension, vascular plant.

Ecotones are transition zones that manifest themselves as sharp or gradual boundaries between bioregions (Clements, 1905, 1916). Spatially, they represent the division of species compositional turnover, driven potentially by varying degrees of environmental discontinuities (Fagan et al., 2003; Liautaud et al., 2020). This spatial variability has been investigated across a spectrum of scales based on field observations, experiments, and correlative modelling (Potts et al., 2015). Within these frameworks, researchers tended to focus on distinct plant community compositions, rather than ecotones as explicit boundaries in themselves. Further, such spatial variation of ecotones has rarely been explored for modelled bioregions, likely due to methodological and data limitations.

In recent years, advances in spatial analytics and tools have enhanced our ability to locate and quantify ecotones (Williams, 1996; Dale, 1999; Fortin et al., 2000; Halley et al., 2004; Hufkens et al., 2009). Traditional methods have incorporated amongst others the moving split window analysis (Hennenberg et al., 2005; Pandita & Dutt, 2020), GIS-based imagery interpretations (Johnston & Bonde, 1989; Müllerová, 2004), wombling (Bowersox & Brown, 2001), and multivariate techniques (Batllori et al., 2009). While these methods have been shown to be effective in detecting the spatial locations of ecotones, they inherently neglect other fundamental boundary characteristics including their shape dynamics.

Characteristically, the shape of ecotones can range from simple to spatially complex (Strayer et al., 2003), and this degree of complexity may be quantified by a fractal dimension (Kenkel & Walker, 1993). As noted by Mandelbrot (1982), the fractal dimension summarizes in a single value the spatial complexities of irregularly shaped features (termed fractals), including those observed in nature (e.g., coastlines and vegetation patterns) (Gao, 2021). The quantification of the fractal dimension relies on the principle of self-similarity in spatial structures across grain sizes, which suggests that when magnified, fractals appear scale invariant (Mandelbrot, 1967, 1982). Through this approach, fractals correspond to fractal dimensions that exceed their topological dimensions. For instance, a jagged boundary

would reflect an intermediate dimension ($1 \leq FD \leq 2$). The higher the fractal dimension, the greater the spatial complexity.

In the context of ecotones, since their boundaries are rarely straight lines (Gastner et al., 2009), and drawing from Mandelbrot (1982), the application of fractal dimension might thus hold promise in enhancing our understanding of ecotone spatial patterns. In that, their fractal dimensions can not only characterize their spatial patterns but also reveal information on the rate of species compositional turnover (Loehle et al., 1996; McGlenn & Palmer, 2011). For instance, lower fractal dimensions are indicative of sharp boundaries with characteristically smoother structures, reflecting sharp changes in species compositions. The shape dynamics of ecotones can occur due to varied environmental discontinuities.

Possible explanations for these discontinuities have been ascribed to climate and topography (Holdridge, 1947; Neilson, 1993; Danz et al., 2011; Hirota et al., 2011; Körner, 2012), geology and soil properties (Muir, 1929; Wiens et al., 1985; Cowling et al., 1997; Goldblatt & Manning, 2002; Rhoades et al., 2005; Esler et al., 2015; Theron et al., 2020), and disturbance factors (Kent et al., 1997; Foggo et al., 2001; Bond et al., 2003; Staver et al., 2011; Pausas et al., 2016). These environmental factors can exert either separate or joint influences on ecotones.

At a biogeographical scale, climate exerts varied temperature-precipitation controls leading to the formation and maintenance of ecotonal boundaries (Will et al., 2013; Erdős et al., 2022). For instance, higher temperatures are a limiting factor to water-dependent plant community compositions, which have greater thermal sensitivities (Toledo et al., 2012; Dulamsuren et al., 2013). By contrast, lower temperatures, particularly in alpine environments, shape the upper limits of ecotones influencing plant distributions in mountainous regions (Walsh et al., 1994; Moen et al., 2008). Precipitation, though spatially variable, is highly influential in shaping plant community compositions leading to ecotone boundaries that are either sharp or gradual (Bond et al., 2003; Sankaran et al., 2005). Given a precipitation gradient, at low and high precipitation

levels we can anticipate sharp boundaries, while gradual boundaries can persist at intermediate levels (e.g., savanna-forest ecotone) (Lehmann et al., 2011; Staver et al., 2011).

Under edaphic conditions mediated by climate (Slesarev et al., 2016; Zhang et al., 2019) sharp ecotonal boundaries can be expected (Marfo et al., 2019; Xue et al., 2019; Eibes et al., 2021). This is likely due to the fact that soils that are highly acidic or alkaline can restrict plant growth and consequently community distributions, through nutrient deficiencies (Kidd & Proctor, 2001), and a reduced water supply to the roots (Lopes et al., 2021).

Disturbances (natural and anthropogenic) impact the structural complexities of plant communities by shaping the composition, density, and spatial distributions of plant species (Turner, 1989). Accentuated by climate and soil factors, the emergence of ecotones has also been attributed to differences in fire regimes (frequency and/or intensity) (Cramer et al., 2018) shaping and maintaining plant species composition and structure (Kruger & Bigalke, 1984; Lavorel & Garnier, 2002; Ónodi et al., 2021). In fire-prone environments, the degree of plant flammability imposes a distributional limit on fire-sensitive plant community composition (Fletcher et al., 2014). An example of this spatial variation is the forest-fynbos ecotone in South Africa (Manders, 1990; Manders & Richardson, 1992).

Using a model-based distribution dataset of more than 23,000 vascular plant species in Africa, we characterize present-day ecotones among vascular plants across mainland sub-Saharan Africa and investigate environmental factors associated with their shapes. Specifically, we explore, (1) whether a fractal dimension is appropriate for characterizing the spatial patterns of present-day ecotones, and (2) how the fractal dimensions of present-day ecotones may vary along latitudes and other environmental contrasts between adjacent bioregions.

MATERIALS AND METHODS

STUDY SYSTEM

Our study was confined to sub-Saharan Africa (Stuart et al., 1990). It extends all of mainland Africa (24 million km²) (Fenta et al., 2020), south of 20°N latitude, and between 20°W and 55°E longitude. Because proximate islands conform to unique ecological processes that differ with mainland (Whittaker et al., 2008), they were excluded.

Sub-Saharan Africa has diverse characteristics of climate, topography, and geology (Wilson & Primack, 2019). The climate is highly variable due to its latitudinal expansion across the northern and southern hemi-

spheres, with the baseline mean annual temperature ranging from 6.22°C to 30.68°C, and the mean annual precipitation ranging from 3.21 to 4320.94 mm (Fick & Hijmans, 2017). Topographical complexities persist in this region (Lamprey, 2021), with prominent peaks recorded in the eastern (Kilimanjaro 5895 m), southern (Thabana-Ntlenyana 3482 m) (Maxted et al., 2004), and western and central (Cameroon 4040 m) parts (Cheek et al., 2021). The soil of a third of the region is naturally acidic (pH < 5.5), owing to poor soil fertility (De Pauw, 1994), characterized by low soil organic matter (Zingore et al., 2015) and clay and silt contents (Bado & Bationo, 2018).

Tremendous plant diversity exists (Klopper et al., 2007) as a result of the region's geography (Catarino & Romeiras, 2020), which has been partitioned into eight major bioregions (Wilson & Primack, 2019), with much of the vegetation flammable (Goldammer & De Ronde, 2004; Bond & Zaloumis, 2016) and getting burnt frequently (Archibald et al., 2010).

SPECIES DATASET

Until recently, data on species distributions of vascular plants in Africa were poorly captured, due to data deficiencies in occurrence records (Küper et al., 2006). Consequently, we utilized a model-based dataset on predicted distributions of 23,189 African vascular plant species of 3616 genera. Considering the reported ~45,000 vascular plants known for sub-Saharan Africa (Klopper et al., 2007), an advantage of this dataset is its comprehensive species list which exceeds earlier studies often restricted to less than 6000 plant species (Linder, 2001; Küper et al., 2004; McClean et al., 2005). This dataset obtained from Conservation International was compiled by the Biodiversity Informatics and Modelling (BIEN) group (<<http://www.biendata.org>>) in the context of the Spatial Planning for Protected Areas in Response to Climate Change (SPARC) project, together with external partners. To produce this dataset, distribution models were fitted using maximum entropy modeling (MaxEnt) (Merow et al., 2019). This approach predicts occurrence probability and relative habitats suitable for species along ecologically relevant environmental gradients (Elith & Leathwick, 2009).

Notably, species occurrence records are typically assembled from various sources in time, space, and taxa, and as a result may be susceptible to biases (Isaac & Poccock, 2015). To mitigate possible spatial and taxonomic biases, the BIEN group, prior to the modeling, spatially thinned the occurrences of each species to 20 km resolution and assessed the validity of taxonomic and geographic locations through BIEN services (Boyle et al., 2013; Merow et al., 2019). The occurrence prob-

ability of each plant species was determined by a suite of environmental predictors for cleaned presence-only records, which was then converted into a binary raster for the fifth percentile (for comprehensive details, see Merow et al., 2019).

CLUSTER ANALYSES

We mapped the binary raster of a species' distribution onto a "fishnet" grid of 20×20 -km cells, using Albers equal area conic projection (WGS1984) in ArcGIS version 10.8.1 with two standard parallels of 20°N and -23°S (ESRI, 2020), which was pruned to cover the entire mainland of sub-Saharan Africa. A site-by-species matrix of presence-absence entries was generated for 55,815 sites using the "raster" R package (Hijmans, 2020; R Core Team, 2021). The species compositional turnover between site-pairs was measured by the Jaccard dissimilarity index (Jaccard, 1900; Podani, 2021) using the "stats" R package (R Core Team, 2021). A nonmetric multidimensional scaling (MDS) was applied based on rank orders (nonmetric) of the derived dissimilarities (Dexter et al., 2018), using the "vegan" R package (Oksanen et al., 2007; R Core Team, 2021). Specifically, species composition in sites were decomposed along three eigenvector dimensions ($k = 3$) to achieve a satisfactory stress value (Oksanen et al., 2007), with stress < 0.05 and < 0.10 considered excellent and good representations of the dissimilarity matrix (Clarke, 1993). Normalized scores of the ordination axes were extracted for mapping species composition in the RGB color scale, with red palette R representing scores along axis 1, green palette G scores of axis 2, and blue palette B scores of axis 3, using the "raster" R package (Hijmans, 2020; R Core Team, 2021). The RGB map was finalized in ArcGIS version 10.8.1 (ESRI, 2020).

The cluster analyses were performed using K-medoids and Clustering Large Applications (CLARA) (Kaufman & Rousseeuw, 1990), based on the site-pair dissimilarities. These algorithms are analogous to K-means, but medoid-based and more robust (less sensitive) to outliers (Kaufman & Rousseeuw, 1990). From these two clustering algorithms, each site was assigned to one cluster (Bishop, 1995). The validity of site partitions was evaluated using the silhouette coefficient (MacQueen, 1967), ranging between -1 and $+1$, with higher values indicating well-supported clusters (Battal & Hennig, 2021). Specifically, the K-medoids and CLARA algorithms were performed 16 times to produce from two to 17 clusters. The partition with the highest silhouette coefficient was chosen for the final optimal number of clusters and best performing algorithm. These analyses were performed using the "cluster" R package (Maechler et al., 2019; R Core Team,

2021). The final cluster results were then mapped using the "raster" R package (Hijmans, 2020; R Core Team, 2021) and finalized in ArcGIS version 10.8.1 (ESRI, 2020).

SPATIAL CHARACTERIZATION OF ECOTONES

We consider ecotones to be boundaries between adjacent bioregions. We converted the map of clusters into vectors using the "rgdal" R package (R Core Team, 2021; Bivand et al., 2022) and extracted the ecotone vectors in ArcGIS version 10.8.1 (ESRI, 2020). We then estimated the fractal dimensions of the present-day ecotone vectors using a custom R code that implements the box-counting fractal dimension method (Mandelbrot, 1982; Klinkenberg, 1994).

Various methods exist to quantify fractal dimensions including the divider relation, power spectrum, and variogram (Kenkel & Walker, 1993; Klinkenberg, 1994; Gao, 2021). In this study, the box-counting fractal dimension method which relies on user-defined box sizes was selected because of its simplicity, computational efficiency, and versatility in analyzing various data types including irregular boundaries.

The general principle of the box-counting fractal dimension method is defined as follows. Given a fractal on a plane (Supplementary Fig. S1), overlay boxes of various sizes and count the number of boxes tracing the fractal feature. The corresponding number of boxes covering the fractal feature declines with the increase of box sizes (Hall & Wood, 1993; Tripathi et al., 2015). The use of different box sizes captures the concept of self-similarity across spatial scales (Mandelbrot, 1967, 1982; Hall & Wood, 1993). Here, since the ecotone vectors were extracted from the 20-km raster of clusters, we considered a series of spatial scales of doubling box sizes ($r = 20, 40, 80, 160, 320, 640, 1280, 2560$ km). Following this procedure, the fractal dimension is then defined by the slope of the natural log-log relationship between the number of boxes covering a fractal feature ($N[r]$) and the linear dimension of the box (r). A strong fit of the log-log relationship corresponds to a true fractal structure characterized by an intermediate dimension (Mandelbrot, 1982).

Using 12 ecologically relevant environmental predictors (Cowling & Potts, 2015; Cramer et al., 2019), we calculated the Spearman's rho correlation (McDonald, 2014) to assess the associations between the fractal dimensions of present-day ecotones and corresponding differences in environmental factors, including differences in average latitude. These differences denoted by the delta symbol (Δ) (see Supplementary Table S1) were computed as the absolute difference in the average values of a particular environmental factor between two adjacent bioregions of an ecotone. This analysis

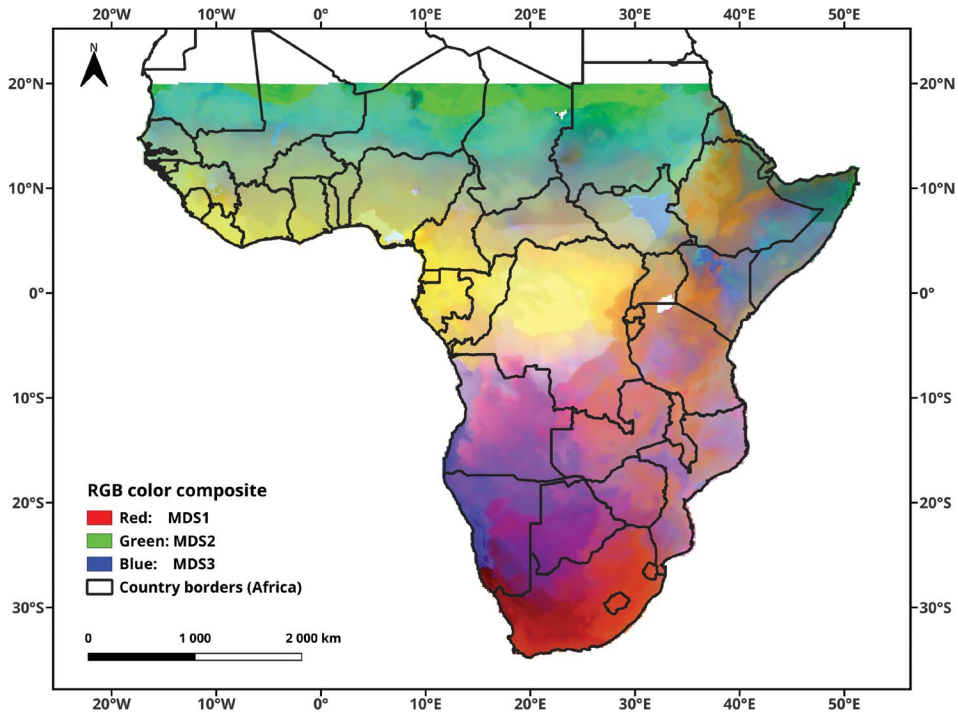


Figure 1. Visual representation of the compositional turnover (measured as the Jaccard dissimilarity) of African vascular plants in mainland sub-Saharan Africa. The RGB color scale reflects normalized scores of the first three multidimensional scaling (MDS) axes; site-pairs sharing similar species composition are depicted by a similar color gradient.

was performed using the base “stats” R package (R Core Team, 2021).

To assess the existence of any nonlinear relationships (Hastie & Tibshirani, 1990), also because the number of measured ecotones is rather low, we fitted a generalized additive model (GAM) between the fractal dimensions of present-day ecotones and each predictor separately, using the “mgcv” R package with the restricted maximum likelihood (REML) method (Wood, 2011; R Core Team, 2021).

RESULTS

The MDS ordination adequately captured sub-Saharan plant species compositional turnover (stress = 0.057) (Fig. 1). The CLARA partitioning algorithm (silhouette coefficient = 0.49; Table 1) outperformed the K-medoids method. This then resulted in seven sub-Saharan bioregions (Fig. 2), which overlapped reasonably well with existing configurations (Olson & Dinerstein, 2002; Linder et al., 2012).

We identified 11 present-day ecotones from the mapped bioregion clusters (Fig. 3). These ecotones represent the optimal boundaries to differentiate within-

Table 1. Clustering validity of two partitioning algorithms for different number of clusters. The silhouette coefficients of the K-medoids and Clustering Large Applications (CLARA) algorithms are shown for $k = 2$ to 17, with the bold value indicating the optimal number of clusters based on the highest silhouette coefficient.

Clusters (k)	Partitioning algorithms	
	K-medoids	CLARA
2	0.43	0.42
3	0.34	0.44
4	0.35	0.39
5	0.37	0.45
6	0.36	0.42
7	0.34	0.49
8	0.37	0.44
9	0.37	0.37
10	0.34	0.46
11	0.35	0.48
12	0.33	0.46
13	0.32	0.41
14	0.33	0.41
15	0.32	0.36
16	0.33	0.37
17	0.33	0.37

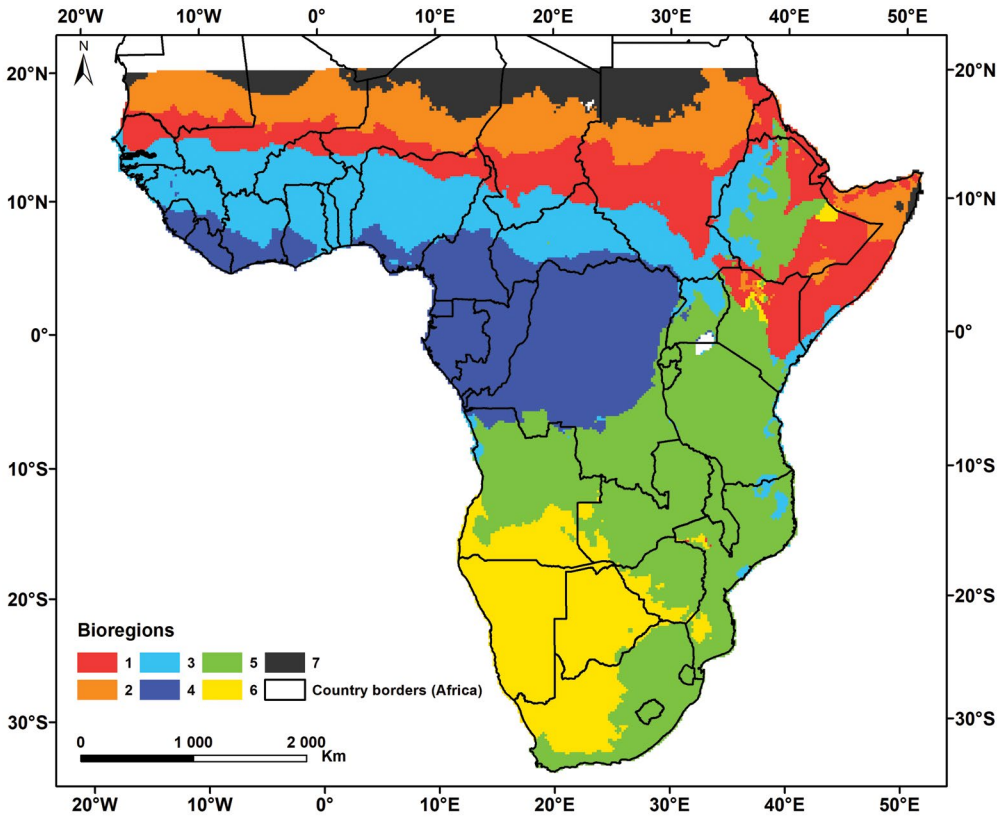


Figure 2. Seven bioregions of African vascular plants spatially distributed across mainland sub-Saharan Africa, based on the Clustering Large Applications (CLARA) partitioning algorithm (silhouette coefficient = 0.49).

versus between-cluster compositional dissimilarity, and their fractal dimensions were measured using the box-counting fractal dimension method (Fig. 4). We removed ecotones that exhibited fractal dimension values of less than one as they represent scattered boundary segments between bioregions. The fractal dimensions of the remaining eight ecotones ranged between 1.018 and 1.154, characterizing relatively sharp boundaries representing clear transitions in plant community compositions.

The associations between the fractal dimensions of the present-day ecotones and the environmental contrasts of adjacent bioregions, including their differences in average latitude, were evaluated using the Spearman's correlation (Table 2), with no statistically significant relationships found. Only the absolute difference in human footprint showed a notable correlation with the fractal dimensions of the present-day ecotones ($\rho = 0.619, P = 0.115$; Table 2).

The GAMs were performed to determine any nonlinear effects of each predictor separately, on the fractal

dimensions of the present-day ecotones. According to the results, only the difference in mean annual precipitation and the fractal dimensions of the present-day ecotones reached significance ($P = 0.02$; Table 3). The deviance explained by this model was 91.2%. The shape of the fractal dimensions of the present-day ecotones follows a unimodal trend with the difference in mean annual precipitation, peaking at an intermediate level of ~ 25 mm and then declining (Fig. 5). This result suggests that with an intermediate difference in mean annual precipitation, higher fractal dimensions of present-day ecotones between bioregions may be observed, contributing to the complexities in the patterning of ecotones. Whereas at > 25 mm in difference in mean annual precipitation, the shape of ecotones may be smoother with lower fractal dimensions. Additionally, the differences between soil organic carbon ($P = 0.0782$) and bulk density ($P = 0.118$) had a near-significant result with the fractal dimensions of the present-day ecotones, with a substantial amount of deviance explained ($> 40\%$; Table 3). A positive linear

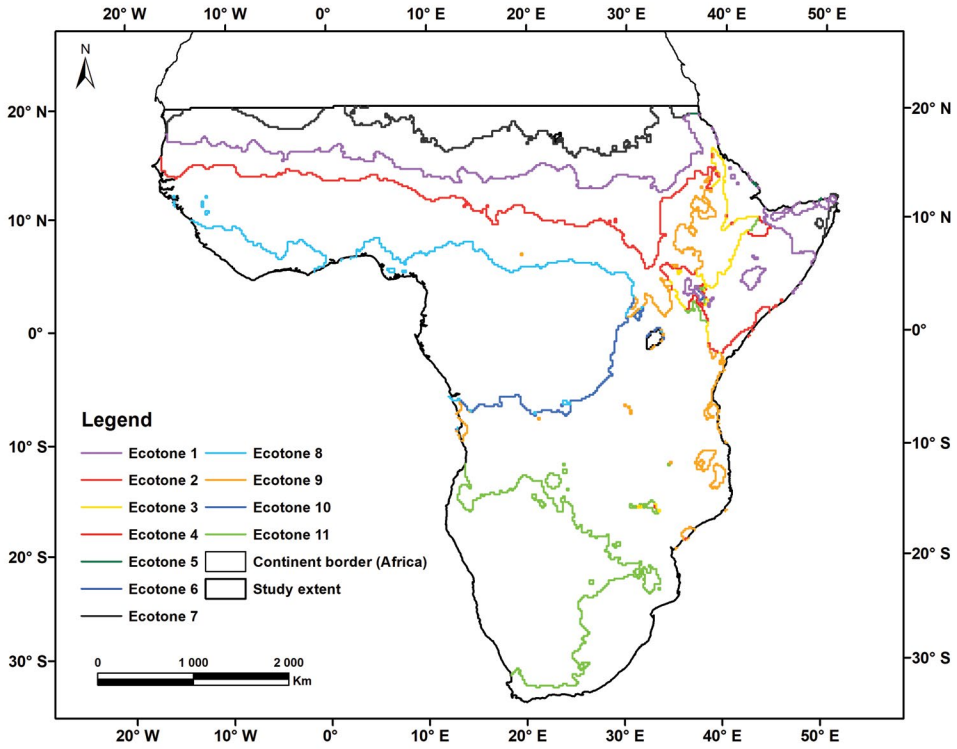


Figure 3. A delineation of present-day ecotones in mainland sub-Saharan Africa, according to boundaries identified between different bioregions.

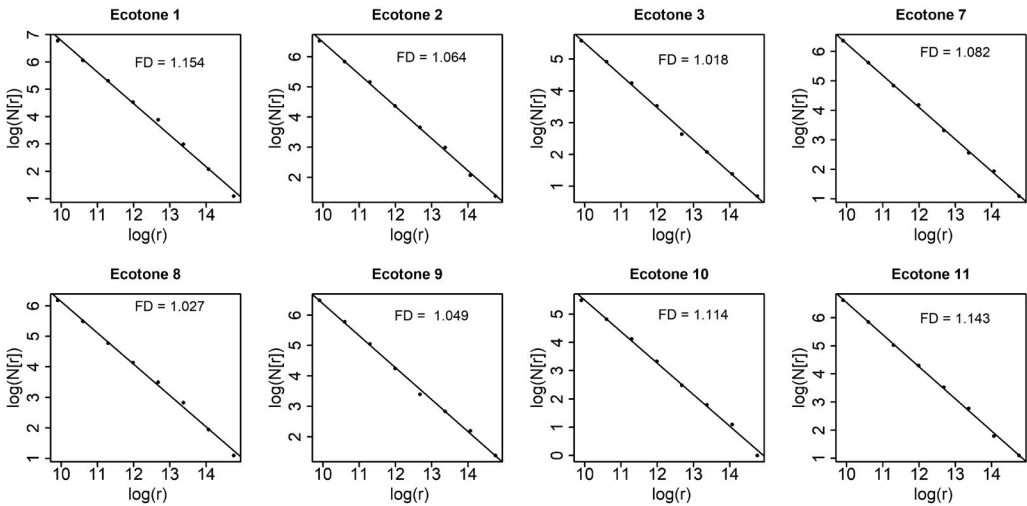


Figure 4. Log-log plots of the box-counting fractal dimension (FD), demonstrating the relationships between the number of boxes covering an ecotone ($N(r)$) and the linear dimension of the box (r). Each slope indicates the fractal dimension of eight present-day ecotones, coinciding with sharp boundaries that reflect characteristically smoother spatial patterns and sharp changes in plant species composition in mainland sub-Saharan Africa.

Table 2. Spearman's rank correlation between differences in environmental factors, including latitudes, and the fractal dimensions of present-day ecotones.

Δ Predictor	Spearman's rho	P value
Δ Mean annual precipitation	-0.5238	0.1966
Δ Mean annual temperature	-0.0238	0.9768
Δ Bulk density	0.1190	0.7930
Δ Soil clay content	0.4048	0.3268
Δ Soil sand content	-0.2619	0.5364
Δ Soil organic carbon	0.5952	0.1323
Δ Soil pH	-0.4286	0.2992
Δ Topographic roughness	-0.0476	0.9349
Δ Fire frequency	-0.0952	0.8401
Δ Human footprint	0.6190	0.1150
Δ Geographic extent	0.1429	0.7520
Δ Latitude	-0.3095	0.4618

effect between the fractal dimensions of the present-day ecotones and the difference in soil organic carbon can be discerned (see Supplementary Fig. S5).

DISCUSSION

Ecotone characterization has traditionally relied on adjacent plant compositions to locate and delineate boundaries along environmental discontinuities, neglecting other fundamental boundary characteristics

Table 3. Statistics of single-predictor generalized additive models, explaining the variation of fractal dimensions among eight present-day ecotones. See Supplementary Table S1 for acronyms of the predictors. The estimated degrees of freedom (edf) indicate the nonlinearity of the smoothed response, with greater values (than one) reflecting more nonlinear relationships.

Predictor	edf	P value	Deviance explained (%)
s(Δ MAP)	3.112	0.0207*	91.2
s(Δ MAT)	1.00	0.894	0.321
s(Δ BD)	2.013	0.118	63.1
s(Δ SCC)	1.633	0.433	34.1
s(Δ SSC)	1.00	0.499	7.95
s(Δ SOC)	1.00	0.0782	42.8
s(Δ PH)	1.467	0.367	34.1
s(Δ TR)	1.00	0.786	1.33
s(Δ FF)	1.00	0.668	3.27
s(Δ HFP)	1.369	0.545	23
s(Δ EXT)	1.00	0.672	3.19
s(Δ LAT)	1.00	0.663	3.39

Signif. codes: 0 '***' 0.001 '**' 0.01 '*' 0.05 '.' 0.1 ' ' 1

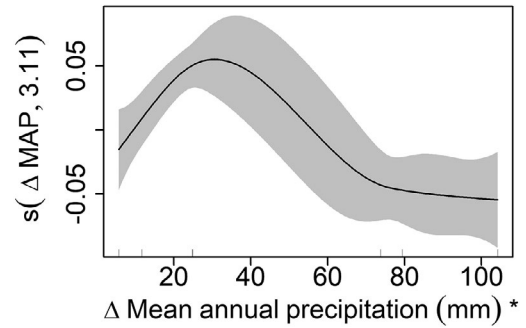


Figure 5. Bivariate plot from the single-predictor generalized additive model (GAM), depicting the response of the fractal dimensions of present-day ecotones to the smoothed absolute difference of mean annual precipitation between adjacent bioregions. Ticks above the horizontal axis indicate the data distribution; shaded areas represent the confidence interval. The asterisk indicates statistical significance.

that reveal information on their structural complexities. Here, we estimated the fractal dimension of ecotones among adjacent African vascular plant bioregions and, in doing so, demonstrated its appropriateness in spatially characterizing ecotones. We further revealed possible explanations of their spatial patterning in present-day mainland sub-Saharan Africa.

BIOREGIONALIZATION

In visualizing the species compositional turnover of 23,189 vascular plants in mainland sub-Saharan Africa for 55,815 sites at 20-km resolution (Fig. 1), we utilized a widely used method (Baldeck & Asner, 2013; Féret & Asner, 2014; Silva & Souza, 2018). From the RGB scale, sites with similar species compositions were indicated by a similar color gradient, leading to a spatial patterning of African plant community compositions with distinct geographic variations latitudinally. By clustering these sites across the entire extent, we found CLARA with seven optimal numbers of clusters to outperform K-medoids (Table 1), revealing its robustness for large datasets; Conradi et al. (2020) reported a similar finding.

The distributions of these compositional clusters exhibited to a degree latitudinal alignments with existing configurations of sub-Saharan bioregions (Olson & Dinerstein, 2002; Linder et al., 2012; Dinerstein et al., 2017). In particular, cluster 4 coincided with the Tropical and Subtropical Moist Broadleaf Forests bioregion, extending slightly beyond the equatorial belt within about 7°N and 7°S (see Supplementary Fig. S2; Olson & Dinerstein, 2002; Dinerstein et al., 2017). The Tropical and Subtropical Grasslands, Savannas, and Shrublands bioregion was largely partitioned into

clusters 1, 2, 3, and 5, respectively, according to the CLARA algorithm. Further, cluster 5 spatially expanded into higher latitudes in the Southern Hemisphere, overlapping with the Montane Grasslands and Shrublands (south-eastward of South Africa) and the Mediterranean Forests, Woodlands, and Scrub bioregions at the southernmost region of Africa. The Deserts and Xeric Shrublands bioregion was seemingly partitioned into clusters 6 and 7, respectively (Supplementary Fig. S2; Olson & Dinerstein, 2002; Dinerstein et al., 2017).

Overall, these spatial congruencies give strength to the species dataset and the partitioning algorithm, reinforcing the robustness of both, respectively. This means that in the context of African conservation of plant diversity, this map product can offer spatial information that may enhance and strengthen existing strategies and plans. In addition, when we explored an alternative number of clusters ($k = 11$; see Table 1), more bioregions and ecotones were identified (Supplementary Fig. S3). These had varied spatial overlaps with the eight existing sub-Saharan bioregions, albeit not maximizing the silhouette coefficient.

ECOTONE SPATIAL CHARACTERIZATION

Given data and methodological limitations, the spatial characterization of ecotones tended to focus on the identification and delineation of boundaries between distinct plant community compositions (Fortin et al., 2000; Morris & Kokhan, 2007). Within this context, a major challenge in traditional ecotone detection methods (see the comprehensive list in Hufkens et al., 2009) has been to consider ecotones as boundaries in themselves. Consequently, their emergence, maintenance factors, and dynamics have typically been understood from the perspective of their adjacent plant communities (e.g., Alados et al., 2003). Therefore, by making use of a fractal dimension, we spatially characterized the shapes of ecotones as explicit boundaries between adjacent bioregions and reported possible explanations of their spatial patterns, corresponding to the rate of plant species compositional turnover in mainland sub-Saharan Africa. To the best of our knowledge, its use in ecotonal research has not yet been explicitly explored.

Research utilizing the application of the fractal dimension has demonstrated its efficacy across various disciplines. Based on the commonly used box-counting fractal dimension method, numerous studies have used the fractal dimension to, for instance, estimate shape complexities of trabeculae (Majumdar et al., 1993), plant morphology (Corbit & Garbary, 1995), urbanized areas (Shen, 2002), and the digital elevation model (DEM) (Taud & Parrot, 2005). Findings from these studies reported high fractal dimensions indicating

greater structural complexities. In contrast, eight of the 11 identified ecotones (Fig. 3) in this study had low fractal dimensions (1.018–1.154) (Fig. 4).

We should note that, to enhance the accuracy of the fractal dimension, a proper selection of the number of box sizes and the scaling factor is needed (Mandelbrot, 1982). To illustrate, in a previous analysis, when only seven box sizes of a scaling factor of two were used, seven of the 11 ecotones were characterized as fractals ranging from 1.025 to 1.143 (Supplementary Fig. S4). This may suggest that the fractal dimension, in principle, may be sensitive to the range of box sizes. This sensitivity, particularly for the box-counting fractal dimension method, has been thoroughly discussed (Dubuc et al., 1989; Liebovitch & Toth, 1989).

When the relationship between fractal dimensions of the eight ecotones were assessed through the Spearman's correlation and the GAMs, only the effect between the difference in mean annual precipitation and the fractal dimensions of the present day was significant ($P = 0.02$, deviance explained = 91.2%; Fig. 5). We also found near-significant (thus weak) effects between the fractal dimensions and differences in human footprint ($P = 0.11$), soil organic carbon ($P = 0.07$), and bulk density ($P = 0.11$), respectively. Although soil pH is well reported as a major determinant of sharp ecotones (Schmiedel & Mucina, 2006; Jolokhava et al., 2020; Theron et al., 2020; Eibes et al., 2021), the potential influence of the organic matter might be worth considering, as it may contribute to our understanding of the emergence and maintenance of gradual transitions of African plant community compositions (Supplementary Fig. S5). All the other analyzed environmental factors including differences in average latitudes were not significant.

The resulting significant unimodal effect of the difference in mean annual precipitation suggests that a moderate gradient of mean annual precipitation may geographically drive the compositional transition of vascular plant communities, captured by the response of the fractal dimensions of present-day ecotones (Fig. 5). This result is consistent with the general prediction that given a moderate change in precipitation, gradual rather than sharp transitions may manifest, leading to a coexistence of water-limited and water-dependent community compositions (Lehmann et al., 2011; Staver et al., 2011; Ciemer et al., 2019). In contrast, with increasing differences in mean annual precipitation between two adjacent bioregions, sharper boundaries with lower fractal dimensions may form (Fig. 5), potentially dividing temperature-driven species in regions with lower precipitation from water-dependent species in regions with higher precipitation (Sankaran et al., 2005; Moreno de las Heras et al., 2015; Bai et al., 2021; Bañares-de-Dios et al., 2022).

CONCLUSION

In this study, we showed that most of the ecotones located between the seven partitioned bioregions across mainland sub-Saharan Africa possess fractal characteristics coinciding with smoother spatial patterns. The fractal dimension can be regarded as an appropriate measure for characterizing the spatial patterns of ecotones. In exploring possible explanations of their shape dynamics, the spatial variation of ecotones is mainly attributed to the gradient of mean annual precipitation. At moderate precipitation, gradual rather than sharp boundaries reinforced by higher fractal dimensions may manifest, promoting coexistence of adjacent plant compositions. At the high end of this gradient, sharp boundaries may persist, corresponding to sharp compositional turnover.

Literature Cited

Alados, C. L., Y. Pueyo, M. L. Giner, T. Navarro, J. Escos, F. Barroso, B. Cabezudo, et al. 2003. Quantitative characterization of the regressive ecological succession by fractal analysis of plant spatial patterns. *Ecol. Model.* 163: 1–17.

Archibald, S., R. J. Scholes, D. P. Roy, G. Roberts & L. Boschetti. 2010. Southern African fire regimes as revealed by remote sensing. *Int. J. Wildland Fire* 19: 861–878.

Bado, V. B. & A. Bationo. 2018. Integrated management of soil fertility and land resources in sub-Saharan Africa: Involving local communities. *Adv. Agron.* 150: 1–33.

Bai, X., W. Zhao, J. Wang & C. S. S. Ferreira. 2021. Precipitation drives the floristic composition and diversity of temperate grasslands in China. *Global Ecol. Conserv.* 32: e01933.

Baldeck, C. & G. Asner. 2013. Estimating vegetation beta diversity from airborne imaging spectroscopy and unsupervised clustering. *Remote Sens.* 5: 2057–2071.

Bañares-de-Dios, G., M. J. Macfa, G. M. de Carvalho, G. Arellano & L. Cayuela. 2022. Soil and climate drive floristic composition in tropical forests: A literature review. *Frontiers Ecol. Evol.* 10: 866905.

Batliori, E., J. M. Blanco-Moreno, J. M. Ninot, E. Gutiérrez & E. Carrillo. 2009. Vegetation patterns at the alpine treeline ecotone: The influence of tree cover on abrupt change in species composition of alpine communities. *J. Veg. Sci.* 20: 814–825.

Batool, F. & C. Hennig. 2021. Clustering with the average silhouette width. *Computat. Statist. Data Analysis* 158: 107190.

Bishop, C. M. 1995. *Neural Networks for Pattern Recognition*. Oxford University Press, Oxford.

Bivand, R., T. Keitt & B. Rowlingson. 2022. Package “Rgdal”: Bindings for the geospatial data abstraction library. Version 1.5–28.

Bond, W. & N. P. Zaloumis. 2016. The deforestation story: Testing for anthropogenic origins of Africa’s flammable grassy biomes. *Philos. Trans. Roy. Soc. B: Biol. Sci.* 371: 20150170.

Bond, W. J., G. F. Midgley & F. I. Woodward. 2003. What controls South African vegetation—Climate or fire? *S. African J. Bot.* 69: 79–91.

Bowersox, M. A. & D. G. Brown. 2001. Measuring the abruptness of patchy ecotones: A simulation-based comparison of landscape pattern statistics. *Pl. Ecol.* 156: 89–103.

Boyle, B., N. Hopkins, Z. Lu, J. A. Raygoza Garay, D. Mozzerin, T. Rees, N. Matasci, et al. 2013. The taxonomic name resolution service: An online tool for automated standardization of plant names. *BMC Bioinform.* 14: 16.

Catarino, L. & M. M. Romeiras. 2020. Biodiversity of vegetation and flora in tropical Africa. *Diversity* 12: 369.

Cheek, M., J. M. Onana & H. M. Chapman. 2021. The montane trees of the Cameroon Highlands, West-Central Africa, with *Deinbollia onanae* sp. nov. (Sapindaceae), a new primate-dispersed, endangered species. *PeerJ* 9: e11036.

Cierner, C., N. Boers, M. Hirota, J. Kurths, F. Müller-Hansen, R. S. Oliveira & R. Winkelmann. 2019. Higher resilience to climatic disturbances in tropical vegetation exposed to more variable rainfall. *Nat. Geosci.* 12: 174–179.

Clarke, K. R. 1993. Non-parametric multivariate analyses of changes in community structure. *Austral. J. Ecol.* 18: 117–143.

Clements, F. E. 1905. *Research Methods in Ecology*. University Publishing Company, Lincoln, Nebraska.

Clements, F. E. 1916. *Plant Succession: An Analysis of the Development of Vegetation*. Carnegie Institution of Washington, Washington, D.C.

Conradi, T., J. A. Slingsby, G. F. Midgley, H. Nottebrock, A. H. Schweiger & S. I. Higgins. 2020. An operational definition of the biome for global change research. *New Phytol.* 227: 1294–1306.

Corbit, J. D. & D. J. Garbary. 1995. Fractal dimension as a quantitative measure of complexity in plant development. *Proc. Roy. Soc. Biol. Sci. Ser. B.* 262: 1–6.

Cowling, R. M. & A. J. Potts. 2015. Climatic, edaphic and fire regime determinants of biome boundaries in the eastern Cape Floristic Region. *S. African J. Bot.* 101: 73–81.

Cowling, R. M., D. M. Richardson & S. M. Pierce (editors). 1997. *Vegetation of Southern Africa*. Cambridge University Press, Cambridge.

Cramer, M. D., S. C. Power, A. Belev, L. Gillson, W. J. Bond, M. T. Hoffman & L. O. Hedin. 2018. Are forest-shrubland mosaics of the Cape Floristic Region an example of alternate stable states? *Ecography* 42: 717–729.

Cramer, M. D., L. M. Wootton, R. van Mazijk & G. A. Verboom. 2019. New regionally modelled soil layers improve prediction of vegetation type relative to that based on global soil models. *Diversity & Distrib.* 25: 1736–1750.

Dale, M. R. T. 1999. *Spatial Pattern Analysis in Plant Ecology*. Cambridge University Press, Cambridge.

Danz, N. P., P. B. Reich, L. E. Frelich & G. J. Niemi. 2011. Vegetation controls vary across space and spatial scale in a historic grassland-forest biome boundary. *Ecography* 34: 402–414.

De Pauw, E. F. 1994. The management of acid soils in Africa. *Outlook Agric.* 23: 11–16.

Dexter, E., G. Rollwagen-Bollens & S. M. Bollens. 2018. The trouble with stress: A flexible method for the evaluation of nonmetric multidimensional scaling. *Limnol. & Oceanogr.: Methods.* 16: 434–443.

Dinerstein, E., D. Olson, A. Joshi, C. Vynne, N. D. Burgess, E. Wikramanayake, N. Hahn, et al. 2017. An ecoregion-based approach to protecting half the terrestrial realm. *BioScience* 67: 534–545.

Dubuc, B., J. F. Quiniou, C. Roques-Carnes, C. Tricot & S. W. Zucker. 1989. Evaluating the fractal dimension of profiles. *Phys. Rev. A.* 39: 1500–1512.

Dulamsuren, C., M. Hauck & C. Leuschner. 2013. Seedling emergence and establishment of *Pinus sylvestris* in the Mongolian forest-steppe ecotone. *Pl. Ecol.* 214: 139–152.

Eibes, P. M., J. Oldeland, S. D. H. Irl, A. Twerski, N. Kühne & U. Schmiedel. 2021. Partitioned beta diversity patterns

- of plants across sharp and distinct boundaries of quartz habitat islands. *J. Veg. Sci.* 32: e13036.
- Elith, J. & J. R. Leathwick. 2009. Species distribution models: Ecological explanation and prediction across space and time. *Annual Rev. Ecol. Evol. Syst.* 40: 677–697.
- Erdős, L., P. Török, J. W. Veldman, Z. Bátor, A. Bede-Fazekas, M. Magnes, G. Kröel-Dulay, et al. 2022. How climate, topography, soils, herbivores, and fire control forest–grassland coexistence in the Eurasian forest-steppe. *Biol. Rev.* 97: 2195–2208.
- Esler, K. J., L. von Staden & G. F. Midgley. 2015. Determinants of the Fynbos/Succulent Karoo biome boundary: Insights from a reciprocal transplant experiment. *S. African J. Bot.* 101: 120–128.
- ESRI. 2020. ArcGIS desktop: Release 10.8.1. Environmental Systems Research Institute, Inc., Redlands, California.
- Fagan, W. F., M. J. Fortin & C. Soykan. 2003. Integrating edge detection and dynamic modelling in quantitative analyses of ecological boundaries. *BioScience* 53: 730–738.
- Fenta, A. A., A. Tsunekawa, N. Haregeweyn, M. Tsubo, H. Yasuda, K. Shimizu, T. Kawai, et al. 2020. Cropland expansion outweighs the monetary effect of declining natural vegetation on ecosystem services in sub-Saharan Africa. *Ecosyst. Serv.* 45: 101154.
- Féret, J. B. & G. P. Asner. 2014. Mapping tropical forest canopy diversity using high-fidelity imaging spectroscopy. *Ecol. Appl.* 24: 1289–1296.
- Fick, S. E. & R. J. Hijmans. 2017. WorldClim 2: New 1-km spatial resolution climate surfaces for global land areas. *Int. J. Climatol.* 37: 4302–4315.
- Fletcher, M. S., S. W. Wood & S. G. Haberle. 2014. A fire-driven shift from forest to non-forest: Evidence for alternative stable states? *Ecology* 95: 2504–2513.
- Foggo, A., C. M. P. Ozanne, R. Speight Martin & C. Hamblen. 2001. Edge effects and tropical forest canopy invertebrates. Pp. 347–359 in K. E. Linsenmair, A. J. Davis, B. Fiala & M. R. Speight (editors), *Tropical Forest Canopies: Ecology and Management*. Springer, Dordrecht.
- Fortin, M. J., R. J. Olson, S. Ferson, L. Iverson, C. Hunsaker, G. Edwards, D. Levine, et al. 2000. Issues related to the detection of boundaries. *Landscape Ecol.* 15: 453–466.
- Gao, J. 2021. *Fundamentals of Spatial Analysis and Modelling*. CRC Press, Boca Raton.
- Gastner, M. T., B. Oborny, D. K. Zimmermann & G. Pruessner. 2009. Transition from connected to fragmented vegetation across an environmental gradient: Scaling laws in ecotone geometry. *Amer. Naturalist* 174: E23–E39.
- Goldammer, J. G. & C. De Ronde (editors). 2004. *Wildland Fire Management Handbook for Sub-Saharan Africa*. Global Fire Monitoring Centre, Freiburg.
- Goldblatt, P. & J. C. Manning. 2002. Plant diversity of the cape region of southern Africa. *Ann. Missouri Bot. Gard.* 89: 281–302.
- Hall, P. & A. Wood. 1993. On the performance of box-counting estimators of fractal dimension. *Biometrika* 80: 246–252.
- Halley, J. M., S. Hartley, A. S. Kallimanis, W. E. Kunin, J. J. Lennon & S. P. Sgardelis. 2004. Uses and abuses of fractal methodology in ecology: Fractal methodology in ecology. *Ecol. Lett.* 7: 254–271.
- Hastie, T. & R. Tibshirani. 1990. *Generalized Additive Models*. Chapman & Hall, Boca Raton.
- Hennerberg, K. J., D. Goetze, L. Kouamé, B. Orthmann & S. Porembski. 2005. Border and ecotone detection by vegetation composition along forest-savanna transects in Ivory Coast. *J. Veg. Sci.* 16: 301–310.
- Hijmans, R. 2020. Package “raster”: Geographic data analysis and modelling. Version 3.3-6.
- Hirota, M., M. Holmgren, E. H. Van Nes & M. Scheffer. 2011. Global resilience of tropical forest and savanna to critical transitions. *Science* 334: 232–235.
- Holdridge, L. R. 1947. Determination of world plant formations from simple climatic data. *Science* 105: 367–368.
- Hufkens, K., P. Scheunders & R. Ceulemans. 2009. Ecotones in vegetation ecology: Methodologies and definitions revisited. *Ecol. Res.* 24: 977–986.
- Isaac, N. J. B. & M. J. O. Pocock. 2015. Bias and information in biological records. *Biol. J. Linn. Soc.* 115: 522–531.
- Jaccard, P. 1900. Contribution au problème de l’immigration post-glaciaire de la flore alpine. *Bull. Soc. Vaud. Sci. Nat.* 36: 87–130.
- Johnston, C. & J. Bonde. 1989. Quantitative analysis of ecotones using a geographic information system. *Photogramm. Engin. Remote Sensing* 55: 1643–1647.
- Jolokhava, T., O. Abdaladze, S. Gadilia & Z. Kikvidze. 2020. Variable soil pH can drive changes in slope aspect preference of plants in alpine desert of the Central Great Caucasus (Kazbegi district, Georgia). *Acta Oecol.* 105: 103582.
- Kaufman, L. & P. J. Rousseeuw. 1990. *Finding Groups in Data: An Introduction to Cluster Analysis*. Wiley, New York.
- Kenkel, N. C. & D. J. Walker. 1993. Fractals and ecology. *Abstr. Bot.* 17: 53–70.
- Kent, M., W. J. Gill, R. E. Weaver & R. P. Armitage. 1997. Landscape and plant community boundaries in biogeography. *Progr. Phys. Geogr.* 21: 315–353.
- Kidd, P. S. & J. Proctor. 2001. Why plants grow poorly on very acid soils: Are ecologists missing the obvious? *J. Exp. Bot.* 52: 791–799.
- Klinkenberg, B. 1994. A review of methods used to determine the fractal dimension of linear features. *Math. Geol.* 26: 23–46.
- Klopper, R. R., L. Gautier, C. Chatelain, G. F. Smith & R. Spichiger. 2007. Floristics of the angiosperm flora of sub-Saharan Africa: An analysis of the African plant checklist and database. *Taxon* 56: 201–208.
- Körner, C. 2012. *Alpine Treelines: Functional Ecology of the Global High Elevation Tree Limits*. Springer, Basel.
- Kruger, F. J. & R. C. Bigalke. 1984. Fire in Fynbos. Pp. 67–114 in P. V. de Booyen & N. M. Tainton (editors), *Ecological Effects of Fire in South African Ecosystems*. Springer, Berlin.
- Küper, W., J. H. Sommer, J. C. Lovett, J. Mutke, H. P. Linder, H. J. Beentje, R. S. A. R. V. Rompaey, et al. 2004. Africa’s hotspots of biodiversity redefined. *Ann. Missouri Bot. Gard.* 91: 525–535.
- Küper, W., J. H. Sommer, J. C. Lovett & W. Barthlott. 2006. Deficiency in African plant distribution data—Missing pieces of the puzzle. *Bot. J. Linn. Soc.* 150: 355–368.
- Lamprey, A. 2021. Tourism, ecosystems, biodiversity and threats. Pp. 35–48 in D. Sparks (editor), *The Blue Economy in Sub-Saharan Africa: Working for a Sustainable Future*. Routledge, London.
- Lavelle, S. & E. Garnier. 2002. Predicting changes in community composition and ecosystem functioning from plant traits: Revisiting the Holy Grail. *Funct. Ecol.* 16: 545–556.
- Lehmann, C. E. R., S. Archibald, W. A. Hoffmann & W. J. Bond. 2011. Deciphering the distribution of the savanna biome. *New Phytol.* 191: 197–209.
- Liautaud, K., M. Barbier & M. Loreau. 2020. Ecotone formation through ecological niche construction: The role of biodiversity and species interactions. *Ecography* 43: 714–723.
- Liebovitch, L. S. & T. Toth. 1989. A fast algorithm to determine fractal dimensions by box counting. *Phys. Lett. A.* 141: 386–390.

- Linder, H. P. 2001. Plant diversity and endemism in sub-Saharan tropical Africa. *J. Biogeogr.* 28: 169–182.
- Linder, H. P., H. M. de Klerk, J. Born, N. D. Burgess, J. Fjeldså & C. Rahbek. 2012. The partitioning of Africa: Statistically defined biogeographical regions in sub-Saharan Africa. *J. Biogeogr.* 39: 1189–1205.
- Loehle, C., B. L. Li & R. C. Sundell. 1996. Forest spread and phase transitions at forest-prairie ecotones in Kansas, U.S.A. *Landscape Ecol.* 11: 225–235.
- Lopes, L. D., J. Hao & D. P. Schachtman. 2021. Alkaline soil pH affects bulk soil, rhizosphere and root endosphere microbiomes of plants growing in a Sandhills ecosystem. *FEMS Microbiol. Ecol.* 97: fiab028.
- MacQueen, J. 1967. Some methods for classification and analysis of multivariate observations. Pp. 281–297 in L. M. Le Cam & J. Neyman (editors), *Proceedings of the Fifth Berkeley Symposium on Mathematical Statistics and Probability*. University of California, Los Angeles.
- Maechler, M., P. Rousseeuw, A. Struyf, M. Hubert & K. Hornik. 2019. Package “cluster”: Cluster analysis basics and extensions. Version 2.1.0.
- Majumdar, S., R. S. Weinstein & R. R. Prasad. 1993. Application of fractal geometry techniques to the study of trabecular bone. *Med. Phys.* 20: 1611–1619.
- Mandelbrot, B. 1967. How long is the coast of Britain? Statistical self-similarity and fractional dimension. *Science* 156: 636–638.
- Mandelbrot, B. 1982. *The Fractal Geometry of Nature*. WH Freeman, New York.
- Manders, P. T. 1990. Fire and other variables as determinants of forest/fynbos boundaries in the Cape Province. *J. Veg. Sci.* 1: 483–490.
- Manders, P. T. & D. M. Richardson. 1992. Colonization of Cape fynbos communities by forest species. *Forest Ecol. Managm.* 48: 277–293.
- Marfo, T. D., R. Datta, S. I. Pathan & V. Vranová. 2019. Ecotone dynamics and stability from soil scientific point of view. *Diversity* 11: 53.
- Maxedt, N., P. Mabuza-Diamini, H. Moss, S. Padulosi, A. Jarvis & L. Guarino. 2004. *An Ecogeographic Study: African Vigna*. Systematic and Ecogeographic Studies of Crop Gene-pools. International Plant Genetic Resources Institute, Rome.
- McClellan, C. J., J. C. Lovett, W. Küper, L. Hannah, J. H. Sommer, W. Barthlott, M. Termansen, et al. 2005. African plant diversity and climate change. *Ann. Missouri Bot. Gard.* 92: 139–152.
- McDonald, J. H. 2014. *Handbook of Biological Statistics*. Sparky House Publishing, Baltimore.
- McGlenn, D. J. & M. W. Palmer. 2011. Quantifying the influence of environmental texture on the rate of species turnover: Evidence from two habitats. *Pl. Ecol.* 212: 495–506.
- Merow, C., B. S. Maitner, H. L. Owens, J. M. Kass, B. J. Enquist, W. Jetz & R. Guralnick. 2019. Species’ range model metadata standards: RMMS. *Global Ecol. Biogeogr.* 28: 1912–1924.
- Moen, J., D. M. Cairns & C. W. Lafon. 2008. Factors structuring the treeline ecotone in Fennoscandia. *Pl. Ecol. Diversity* 1: 77–87.
- Moreno de las Heras, M., R. Diaz-Sierra, L. Turnbull & J. Wainwright. 2015. Assessing vegetation structure and ANPP dynamics in a grassland–shrubland Chihuahuan ecotone using NDVI–rainfall relationships. *Biogeosciences* 12: 2907–2925.
- Morris, A. & S. Kokhan (editors). 2007. *Geographic Uncertainty in Environmental Security*. Springer, Dordrecht.
- Muir, J. 1929. The Vegetation of the Riversdale Area, Cape Province. *Mem. Bot. Surv. S. Africa* 13: 1–82.
- Müllerová, J. 2004. Use of digital aerial photography for sub-alpine vegetation mapping: A case study from the Krkonoše Mts., Czech Republic. *Pl. Ecol.* 175: 259–272.
- Neilson, R. P. 1993. Transient ecotone response to climatic change: Some conceptual and modelling approaches. *Ecol. Appl.* 3: 385–395.
- Oksanen, J., R. Kindt, P. Legendre, B. O’Hara, M. H. H. Stevens & M. J. Oksanen. 2007. Package “vegan”: Community ecology package. Version 2.5-6.
- Olson, D. & E. Dinerstein. 2002. The Global 200: Priority ecoregions for global conservation. *Ann. Missouri Bot. Gard.* 89: 199–224.
- Ónodi, G., M. Kertész, A. Lengyel, I. Pándi, L. Somay, K. Sztár & G. Kröel-Dulay. 2021. The effects of woody plant encroachment and wildfire on plant species richness and composition: Temporal changes in a forest–steppe mosaic. *Appl. Veg. Sci.* 24: e12546.
- Pandita, S. & H. C. Dutt. 2020. Land use induced blurring of forest-grassland transition in north-west Himalaya—A case study using moving split window boundary detection technique. *J. Mountain Sci.* 17: 3085–3096.
- Pausas, J. G., R. B. Pratt, J. E. Keeley, A. L. Jacobsen, A. R. Ramirez, A. Vilagrosa, S. Paula, et al. 2016. Towards understanding resprouting at the global scale. *New Phytol.* 209: 945–954.
- Podani, J. 2021. The wonder of the Jaccard coefficient: From alpine floras to bipartite networks. *Fl. Medit.* 31: 105–123.
- Potts, A. J., G. R. Moncrieff, W. J. Bond & R. M. Cowling. 2015. An operational framework for biome boundary research with examples from South Africa. *S. African J. Bot.* 101: 5–15.
- R Core Team. 2021. R: A language and environment for statistical computing. R Foundation for Statistical Computing, Vienna.
- Rhoades, C. C., S. P. Miller & D. L. Skinner. 2005. Forest vegetation and soil patterns across glade-forest ecotones in the Knobs region of Northeastern Kentucky, USA. *Amer. Midl. Naturalist* 154: 1–10.
- Sankaran, M., N. P. Hanan, R. J. Scholes, J. Ratnam, D. J. Augustine, B. S. Cade, J. Gignoux, et al. 2005. Determinants of woody cover in African savannas. *Nature* 438: 846–849.
- Schmiedel, U. & L. Mucina. 2006. Vegetation of quartz fields in the Little Karoo, Tanqua Karoo and eastern Overberg (Western Cape Province, South Africa). *Phytocoenologia* 36: 1–44.
- Shen, G. 2002. Fractal dimension and fractal growth of urbanized areas. *Int. J. Geogr. Inform. Sci.* 16: 419–437.
- Silva, A. C. & A. F. Souza. 2018. Aridity drives plant biogeographical sub regions in the Caatinga, the largest tropical dry forest and woodland block in South America. *PLoS One* 13: e0196130.
- Slessarev, E. W., Y. Lin, N. L. Bingham, J. E. Johnson, Y. Dai, J. P. Schimel & O. A. Chadwick. 2016. Water balance creates a threshold in soil pH at the global scale. *Nature* 540: 567–569.
- Staver, A. C., S. Archibald & S. A. Levin. 2011. The global extent and determinants of savanna and forest as alternative biome states. *Science* 334: 230–232.
- Strayer, D. L., M. E. Power, W. F. Fagan, S. T. A. Pickett & J. Belnap. 2003. A classification of ecological boundaries. *BioScience* 53: 723–729.
- Stuart, S. N., R. J. Adams & M. D. Jenkins. 1990. Biodiversity in Sub-Saharan Africa and Its Islands: Conservation, Management, and Sustainable Use. IUCN, Gland.
- Taud, H. & J. F. Parrot. 2005. Measurement of DEM roughness using the local fractal dimension. *Geomorphol. Relief Processes Environm.* 11: 327–338.

- Theron, E. J., A. C. van Aardt & P. J. du Preez. 2020. Vegetation distribution along a granite catena, southern Kruger National Park, South Africa. *Koedoe* 62: 1–11.
- Toledo, M., M. Peña-Claros, F. Bongers, A. Alarcón, J. Balcázar, J. Chuvina, C. Leño, et al. 2012. Distribution patterns of tropical woody species in response to climatic and edaphic gradients. *J. Ecol.* 100: 253–263.
- Tripathi, S. K., C. P. Kushwaha, A. Roy & S. K. Basu. 2015. Measuring ecosystem patterns and processes through fractals. *Curr. Sci.* 109: 1418–1426.
- Turner, M. G. 1989. Landscape ecology: The effect of pattern on process. *Annual Rev. Ecol. Evol. Syst.* 20: 171–197.
- Walsh, S. J., D. R. Butler, T. R. Allen & G. P. Malanson. 1994. Influence of snow patterns and snow avalanches on the alpine treeline ecotone. *J. Veg. Sci.* 5: 657–672.
- Whittaker, R. J., K. A. Triantis & R. J. Ladle. 2008. Original article: A general dynamic theory of oceanic island biogeography. *J. Biogeogr.* 35: 977–994.
- Wiens, J. A., C. S. Crawford & J. R. Gosz. 1985. Boundary dynamics: A conceptual framework for studying landscape ecosystems. *Oikos* 45: 421–427.
- Will, R. E., S. M. Wilson, C. B. Zou & T. C. Hennessey. 2013. Increased vapor pressure deficit due to higher temperature leads to greater transpiration and faster mortality during drought for tree seedlings common to the forest–grassland ecotone. *New Phytol.* 200: 366–374.
- Williams, P. H. 1996. Mapping variations in the strength and breadth of biogeographic transition zones using species turnover. *Proc. Roy. Soc. Biol. Sci. Ser. B.* 263: 579–588.
- Wilson, J. W. & R. B. Primack. 2019. *Conservation Biology in Sub-Saharan Africa*. Open Book Publishers, Cambridge.
- Wood, S. N. 2011. Fast stable restricted maximum likelihood and marginal likelihood estimation of semiparametric generalized linear models. *J. Roy. Statist. Soc. B: Statist. Methodol.* 73: 3–36.
- Xue, W., T. M. Bezemer & F. Berendse. 2019. Soil heterogeneity and plant species diversity in experimental grassland communities: Contrasting effects of soil nutrients and pH at different spatial scales. *Pl. Soil* 442: 497–509.
- Zhang, Y. Y., W. Wu & H. Liu. 2019. Factors affecting variations of soil pH in different horizons in hilly regions. *PLoS One* 14: e0218563.
- Zingore, S., J. Mutegi, B. Agesa, L. Tamene & J. Kihara. 2015. Soil degradation in sub-Saharan Africa and crop production options for soil rehabilitation. *Better Crops* 99: 24–26.